© 2018. Published by The Company of Biologists Ltd | Development (2018) 145, dev164335. doi:10.1242/dev.164335

STEM CELLS AND REGENERATION

RESEARCH REPORT

Clonal analysis reveals laminar fate multipotency and daughter cell apoptosis of mouse cortical intermediate progenitors

Anca B. Mihalas[1,*] and Robert F. Hevner[1,2,‡,§]

ABSTRACT

In developing cerebral cortex, most pyramidal-projection neurons are produced by intermediate progenitors (IPs), derived in turn from radial glial progenitors. Although IPs produce neurons for all cortical layers, it is unknown whether individual IPs produce multiple or single laminar fates, and the potential of IPs for extended proliferation remains uncertain. Previously, we found that, at the population level, early IPs (present during lower-layer neurogenesis) produce lower- and upper-layer neurons, whereas late IPs produce upper-layer neurons only. Here, we employed mosaic analysis with double markers (MADM) in mice to sparsely label early IP clones. Most early IPs produced 1-2 neurons for deep layers only. Less frequently, early IPs produced larger clones (up to 12 neurons) spanning lower and upper layers, or upper layers only. The majority of IP-derived clones (~66%) were associated with asymmetric cell death after the first division. These data demonstrate that laminar fate is not predetermined, at least in some IPs. Rather, the heterogeneous sizes and laminar fates of early IP clones are correlated with cell division/death/differentiation choices and neuron birthdays, respectively.

KEY WORDS: Tbr2, Intermediate progenitors, Mosaic analysis with double markers, MADM, Cortical development, Laminar fate

INTRODUCTION

Intermediate progenitors (IPs) produce glutamatergic projection neurons for all cortical layers (Kowalczyk et al., 2009; Vasistha et al., 2015; Mihalas et al., 2016). However, the mechanisms and timing of laminar fate determination in IPs are still uncertain. The progressive fate restriction model holds that radial glial progenitors (RGPs) are initially multipotent for laminar fate, but gradually lose the ability to generate deep cortical layers, produced earlier in the 'inside-out' neurogenic sequence (Leone et al., 2008). In contrast, the early-fate restriction model postulates that RGPs become predetermined to produce specific neuron subtypes, such as upper layers, at the onset of neurogenesis (Franco et al., 2012).

The laminar fates of IPs, which are derived from RGPs, have important implications for understanding mechanisms of laminar fate specification and amplification of neurogenesis. Previously, genetic fate mapping of Tbr2^{+} (Eomes^{+} – Mouse Genome Informatics) IPs revealed a significant cohort of early IP-derived neurons (~17%) that occupied upper cortical layers (Mihalas et al., 2016). Significantly, these early IP-derived upper-layer neurons were born late in corticogenesis, indicating that some early IP lineages did not immediately differentiate as neurons, but continued proliferating or remained quiescent until late neurogenesis; or divided asymmetrically to produce both lower and upper layers. We hypothesized that early IPs are multipotent for laminar fate, not only as a population, but also within individual IP clones.

To label IP-derived clones, we used mosaic analysis with double markers (MADM) in mice (Hippenmeyer et al., 2010). With this sparse labeling method, we could determine clone sizes and laminar fates of early IPs with high confidence. Previous studies using different methods have reported disparate observations concerning IP clone sizes, ranging from 2 to 4 neurons (Noctor et al., 2004; Gao et al., 2014), to 4 to 8 neurons (Wu et al., 2005), to as many as 32 neurons (Vasistha et al., 2015). Using MADM, we sought to precisely define individual clone sizes and fates, and to test the hypothesis that individual IPs can produce multiple laminar identities.

The MADM method of genetic lineage tracing relies on combining a cell type-specific Cre recombinase with a sensitive MADM reporter. Here, we used *Tbr2*^{CreER} (*Eomes*^{CreERT2}) to specifically trace IPs (Pimeisl et al., 2013; Mihalas et al., 2016). Tbr2 is an IP-specific transcription factor involved in the differentiation of glutamatergic neurons (Englund et al., 2005; Hevner et al., 2006; Kawaguchi et al., 2008; Mihalas et al., 2016). For the reporter, we used *Madm11* mice, known to produce effective labeling of clones in cerebral cortex (Hippenmeyer et al., 2010; Gao et al., 2014). Upon injection of the CreER-activating ligand, tamoxifen, IPs and their progeny were permanently labeled, with each IP daughter cell (and their progeny) expressing a different fluorophore: either TdTomato, a red fluorescent protein (RFP); or enhanced green fluorescent protein (GFP).

From this clonal analysis, several findings emerged: (1) the majority of early IPs (~90%) produce deep-layer clones by rapid differentiation; (2) a minority of early IPs produce multilayer or upper-layer clones; (3) the average clone size of early IPs is ~2 neurons (2.3±0.4), although most clones are smaller; (4) IP daughter neurons generated simultaneously have identical (symmetric) laminar fates; (5) many IP primary daughter cells undergo cell death, yielding single-color (RFP^{+} or GFP^{+}) clones by MADM, sometimes consisting of a single neuron; and (6) multilayer clones were all single color, suggesting that these larger clones might require a binary cell death decision, as described in other systems. Thus, early IPs produce heterogeneous laminar fates and clone sizes, and some IPs are multipotent with regard to laminar fate.

RESULTS AND DISCUSSION

IP clones are sparsely labeled with *Tbr2*^{CreER} and MADM

To produce neuron clones from early IPs in mice, we combined inducible genetic lineage tracing driven by *Tbr2*^{CreER} (also known

[1]Center for Integrative Brain Research, Seattle Children's Research Institute, Seattle, WA 98101, USA. [2]Department of Neurological Surgery, University of Washington School of Medicine, Seattle, WA 98104, USA.
*Present address: Department of Neurological Surgery, University of Washington, Seattle, WA, USA. ‡Present address: Department of Pathology, University of California, San Diego, La Jolla, CA, USA.

§Author for correspondence (rhevner@ucsd.edu)

R.F.H., 0000-0002-8441-1047

Received 7 February 2018; Accepted 29 July 2018

Development (2018) 145, dev164335. doi:10.1242/dev.164335

as *Eomes*^{CreERT2}; Pimeisl et al., 2013), with the MADM system for clonal labeling of dividing cells, to differentially label sister cell progenies with red and green fluorescent reporters (Hippenmeyer et al., 2010). Specifically, *Tbr2*^{CreER};*Madm11*$^{GT/GT}$ males were bred with *Madm11*$^{TG/TG}$ females, and pregnant dams were injected with tamoxifen to activate CreER on embryonic day (E) 11.5, E12.5 or E13.5. Embryos were studied after survival to E18.5-E19.5, allowing for IP proliferation, neuronal differentiation and migration (Fig. 1A). Postnatal survival was not feasible in this system because of perinatal mortality related to dystocia (Mihalas et al., 2016; Kaplan et al., 2017). Nevertheless, analysis on E18.5-E19.5 is expected to accurately determine the laminar fates of most early IP-derived neurons, because only a minority of late-born neurons are still migrating around the time of birth (Hevner et al., 2004). Accordingly, the laminar fates of neurons traced from early RGPs appear similar after analysis on E19.5 or postnatal day 7 (Kaplan et al., 2017).

In this inducible genetic system, tamoxifen activates CreER in cells that express, or recently expressed, the *Tbr2* gene (Pimeisl et al., 2013; Mihalas et al., 2016). Because *Tbr2* is expressed only in IPs, and not in RGPs (Englund et al., 2005; Kawaguchi et al., 2008; Kaplan et al., 2017), tamoxifen activates CreER specifically in IPs at the time of tamoxifen administration (Mihalas et al., 2016). Upon CreER activation, *Madm* loci undergo recombination in dividing and quiescent cells, with distinct outcomes (Hippenmeyer et al., 2010). In mitotic X-segregation (analyzed in the present study), one daughter cell is labeled with tdTomato (RFP) and the other with GFP (Fig. 1B). In mitotic Z-segregation, one daughter cell is labeled yellow (RFP$^+$/GFP$^+$) and the other is unlabeled. Also, quiescent (G0/G1) recombination labels one cell yellow. Because cells can be labeled yellow without mitosis, the present analysis was restricted to green and/or red clones, produced by IP mitosis with X-segregation (Fig. 1B). At the tamoxifen dosage used, submaximal activation of CreER caused recombination in a small subset of *Tbr2*-expressing cells, leading to sparse labeling of IP-derived clones.

Early IP-derived neuron clones exhibit heterogeneous sizes and laminar fates

Analysis of 41 neocortical clones from 24 embryos revealed several patterns of clonal expansion and laminar fates. The most frequently observed type of clone consisted of a single neuron, either GFP$^+$ (green) or RFP$^+$ (red), in layer 6, presumably arising by IP division with one daughter cell undergoing apoptosis (Fig. 2A). Also frequently observed were clones consisting of a pair of neurons, one GFP$^+$ and one RFP$^+$, in layer 6 (Figs 1D and 2A). This type of clone was presumably derived by symmetric division of an early IP, to generate a pair of early-born (deep layer) neurons (‘Neurogenic’ in Fig. 1B).

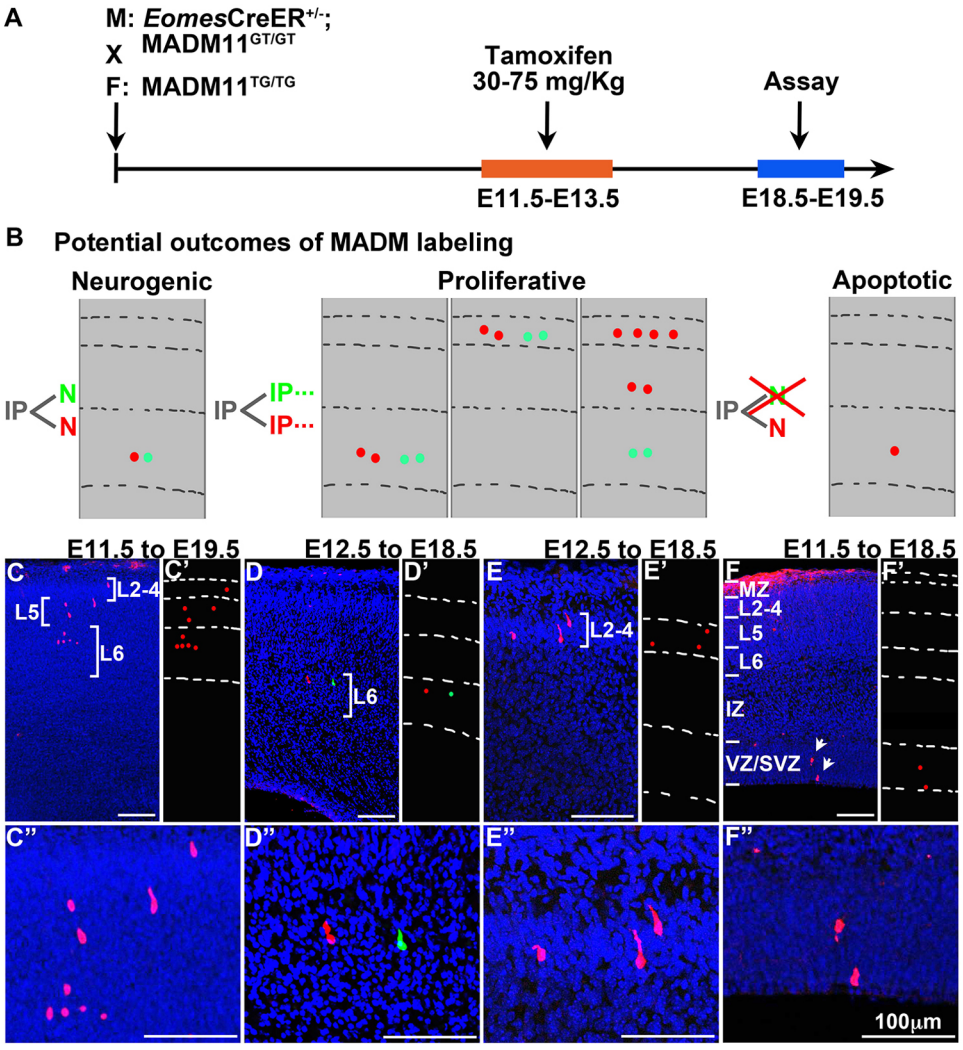

Fig. 1. Early IPs generate single- and multilayered clones of neurons. (A) Experimental design timeline. (B) Diagrams of potential IP-derived clonal outcome by MADM labeling. Yellow clones were excluded (see text). (C) Confocal microscopy image of E19.5 cortex after tamoxifen injection at E11.5. A 9-neuron RFP$^+$-only clone spanned layers 2-6. (D) Confocal microscopy image of E18.5 cortex after tamoxifen injection at E12.5. A 2-cell clone contained one RFP$^+$ and one GFP$^+$ neuron in layer 6. (E) Confocal microscopy image of E18.5 cortex after tamoxifen injection at E12.5. A 3-neuron, RFP$^+$-only clone occupied upper layers. (F) Confocal microscopy image of E18.5 cortex after tamoxifen injection at E11.5. Sister cells in VZ/SVZ exhibited IP morphologies (Kowalczyk et al., 2009). (C′-F′) Schematic diagrams of the clones in C-F. (C″-F″) Higher magnification views of the clones in C-F. Scale bars: 100 µm. IZ, intermediate zone; L, layer; MZ, marginal zone; SVZ, subventricular zone; VZ, ventricular zone.

Development (2018) 145, dev164335. doi:10.1242/dev.164335

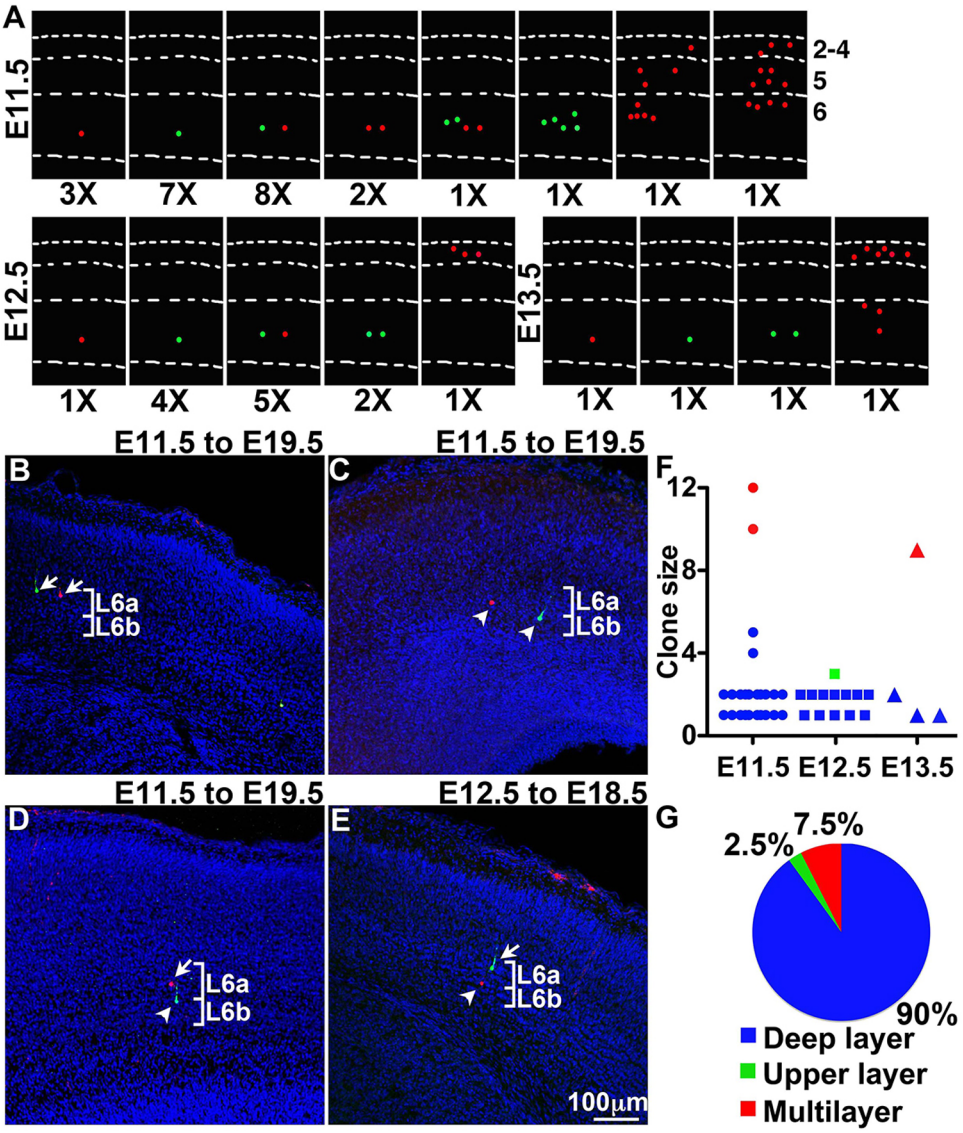

Fig. 2. Neuronal composition of 41 IP-derived clones. (A) Schematic diagrams of all 41 evaluable neocortical clones, indicating the distribution of neurons in each layer. The 'X' under each diagram indicates how many clones exhibited the indicated neuron number and laminar distribution. (B) Confocal microscopy image of E19.5 cortex after tamoxifen injection at E11.5. Clone consisted of one RFP^+ and one GFP^+ neuron, both in layer 6a (arrows). (C) Confocal microscopy image of E19.5 cortex after tamoxifen injection at E11.5. Clone consisted of one RFP^+ and one GFP^+ neuron, both in layer 6b (arrowheads). (D) Confocal microscopy image of E19.5 cortex after tamoxifen injection at E11.5. Clone consisted of one RFP^+ and one GFP^+ neuron, in layers 6a (arrow) and 6b (arrowhead), respectively. (E) Confocal microscopy image of E18.5 cortex after tamoxifen injection on E12.5. Clone consisted of one GFP^+ and one RFP^+ neuron, in layers 6a (arrow) and 6b (arrowhead), respectively. (F) Plot of IP-derived clone size. (G) Pie chart depicting the percentage clonal distribution within the various layers of the 6-layer neocortex.

We also found larger clones, that were restricted to a single cortical layer, or that spanned multiple layers (Figs 1C and 2A). The average size of multilayer clones was 10±1 neurons (n=3 clones, from E11.5 to E13.5 combined), and they comprised ~7.5% (3/41) of all early IP clones. Whereas clones located within the same cortical layer exhibited negligible cell dispersion, multilayer clones spanned multiple serial sections, occupying larger volumes. To confirm the clonal relationship of neurons in multilayer groups, we applied nearest-neighbor distance (NND) analysis (Brown et al., 2011; Gao et al., 2014). The NNDs of neurons in multilayer clones were significantly shorter than those of simulated random distributions, supporting the presumption of clonality (Fig. S1; $P<5\times10^{-4}$ for all 3 multilayer clones).

Interestingly, all 3 multilayer clones also consisted of neurons of only one color (red or green), indicating that they were derived from one daughter cell of an early IP division, with the other daughter cell presumably undergoing apoptosis. Moreover, 5 of 6 clones (83%) larger than 2 cells were single color, while among 1- or 2-cell clones, only 22 of 35 (63%) were single color. Together, the results indicate that apoptosis of one daughter cell is overall a common outcome after division of early IPs (27/41; 66%), and suggest that apoptosis of one IP daughter cell might be important to generate large or multilayer clones. However, the number of observations was too small to prove the latter point statistically (P>0.05, chi-squared test).

The high rate of early IP daughter cell death observed here is consistent with previous studies showing abundant programmed cell death in progenitor zones of developing neocortex, especially the subventricular zone (SVZ), affecting up to 67-70% of recently divided cells (Blaschke et al., 1996; Thomaidou et al., 1997). Although these previous studies reported somewhat different rates of cell death, both identified the SVZ as an important site of apoptosis. Our observations in the present study appear to support a relatively high rate of apoptosis, as found by Blaschke et al. (1996), at least among IP daughter cells.

As expected, the majority of early IP-derived clones (90%) occupied deep layers only (Fig. 2F,G). Just one upper layer-only clone was observed (Figs 1E and 2A,G), evidently derived from an early IP, the surviving progeny of which did not undergo final neurogenic divisions until several days later, during upper-layer neurogenesis (Fig. 3B3). Because this clone was single color, we cannot rule out that the other IP daughter cell (lost by apoptosis) might have been specified to generate deep-layer neurons. Thus,

Development (2018) 145, dev164335. doi:10.1242/dev.164335

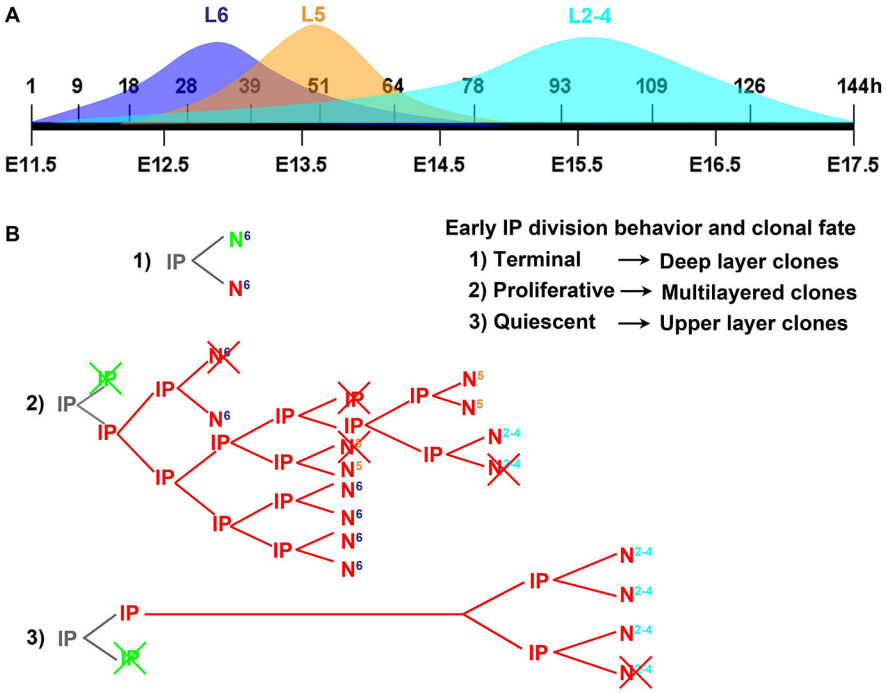

Fig. 3. Inferred pathways of early IP division, death and laminar differentiation. (A) Sequence of laminar neurogenesis in mouse neocortex (Caviness et al., 2003; Hevner et al., 2003). (B) Three examples of early IP division behavior and clonal fate, inferred from lineage tracing. (1) An early IP terminal division pattern leading to a red and green L6 clone (see Fig. 1D). (2) Potential model for genesis of a multilayered red-only clone (see Fig. 1C). (3) Potential model for genesis of an upper-layer red-only clone (see Fig. 1E). h, hours; N^n, neuron (superscript 'n' indicates the cortical layer location); gray 'IP' indicates the founder IP of a clone; red or green 'N' or 'IP' indicate fluorophore segregation within cells after MADM labeling.

although this IP-derived clone consisted of only upper-layer neurons, it might not have been upper-layer restricted. Interestingly, one clone consisted of a pair of RFP^+ cells with short processes, morphologically typical of IPs, in the ventricular zone (VZ) and SVZ on E18.5 (Fig. 1F). These presumed IPs were poised for differentiation during the final stage of neurogenesis (Fig. 3A), to generate upper-layer neurons (Fig. 3B3).

Overall, these results demonstrate 3 main types of early IP clonal differentiation (Fig. 3B): (1) rapid terminal division after 1-2 mitotic cycles to produce deep-layer neurons; (2) division with asymmetric laminar fates to produce multilayered clones; or (3) division with delayed terminal differentiation to produce upper-layer neurons. Asymmetric cell death of IP daughter cells was observed in conjunction with all of these modes of division (Fig. 2A).

To determine whether IPs undergoing terminal differentiation could produce sister neurons destined for different layers, we examined the laminar fates of 2-cell clones consisting of one RFP^+ neuron and one GFP^+ neuron. In all such clones, the 2 daughter neurons were located in the same cortical layer (Fig. 2A). Within layer 6, which has sublaminae 6a and 6b (subplate), some neuron pairs resided together in the same sublamina (Fig. 2B,C), whereas in other clones, the 2 daughter neurons appeared to occupy different sublaminae (Fig. 2D,E). These data demonstrated that layers 6a and 6b can contain sister neurons, although further studies will be necessary to evaluate whether such pairs consist of different neuron subtypes, or the same subtype distributed into different sublaminae (Hevner et al., 2003; Hoerder-Suabedissen and Molnár, 2013).

IP clonal analysis is most consistent with the progressive restriction model

The progressive restriction model posits that cortical projection neuron subtype is determined by factors in the VZ/SVZ when neurons are born, and by the intrinsic laminar fate potential of RGPs, progressively restricted to more superficial layers as neurogenesis proceeds (McConnell, 1985; Luskin et al., 1988; Walsh and Cepko, 1988; McConnell and Kaznowski, 1991; Desai and McConnell, 2000; Shen et al., 2006; Leone et al., 2008). In contrast, the early commitment model proposes that a subset of RGPs, such as those expressing *Cux2*, are committed to produce upper-layer neurons only, even at the onset of neurogenesis (Franco et al., 2012). The early commitment and progressive restriction models are not mutually exclusive, as they can conceivably operate in parallel in different RGP clones, but the phenomenon of early commitment remains controversial (Guo et al., 2013; Gao et al., 2014; Eckler et al., 2015; Gil-Sanz et al., 2015).

In the present study, we found that the vast majority of early IPs differentiate rapidly to produce 1-4 deep-layer neurons, but a subset (5-10%) continue proliferating to produce larger clones, and sometimes contribute to upper-layer neurogenesis (Figs 1C-C″,E-E″ and 2F,G). Rarely, some early IP clones can even remain progenitors from early to late neurogenesis (Fig. 1F). Our results also imply that at least some early IPs retain laminar fate multipotency, as revealed in multilayer clones (Figs 1C-C″ and 2A). In any case, the neurons derived from IPs invariably maintain the classic 'inside-out' relationship between laminar fate and cell birthday (Mihalas et al., 2016). Together, these results suggest that early IPs undergo differentiation or (less often) proliferation on a stochastic basis, and produce neurons with lower- or upper-layer identity according to cell birthday.

Relevant to the early commitment model, only a single clone of upper layer-only neurons was observed, representing just ∼2.5% of early IP clonal outcomes (Figs 1E-E″ and 2G). Upper layer-only clones could potentially be produced from multipotent early IPs by proliferation without genesis of lower-layer neurons (perhaps due to apoptosis of daughter cells destined for lower layers), or by IP genesis from upper layer-restricted RGPs that impart upper-layer restriction on their IP progeny. If such upper layer-restricted RGPs are present in early neocortex, our data indicate they are either very low abundance (estimated <5%), or produce early IPs only rarely.

Heterogeneity of IPs and binary cell death decisions might regulate clonal expansion

Previous studies using various methods have observed different degrees of IP clonal expansion. Using CLoNe, a method based on

Development (2018) 145, dev164335. doi:10.1242/dev.164335

inducible fluorophores and *in utero* electroporation, Vasistha et al. (2015) found that IPs produced large clones (8-16 neurons) more frequently than small clones (1-8 neurons); in particular, early IPs produced very large clones (16-32 neurons). In contrast, clonal analysis of RGP lineages by MADM implied that IPs (inferred from lineage trees) produce clones of 2 neurons (Gao et al., 2014). Another method, *Nex* (*Neurod6*)-Cre retroviral lineage tracing, determined that IPs can produce up to 8 cells per clone during midneurogenesis (Wu et al., 2005). In the present study, most IP-derived clones were small (1-2 neurons), but larger clones (up to 12 neurons) were also observed (Fig. 2F). Early IPs thus exhibited relatively low proliferative potential overall, along with high levels of apoptosis of primary daughter cells (single-color clones), as compared with early RGPs (Gao et al., 2014; Kaplan et al., 2017).

One potential mechanism for regulating IP proliferation could involve the differential expression of transcription factors, such as Pax6, expressed in ∼25% of Tbr2^{+} IPs in E14.5 mouse neocortex (Englund et al., 2005). Indeed, it has been proposed that Pax6^{+} IPs are proliferative, whereas Pax6^{-} IPs are neurogenic (Florio and Huttner, 2014). However, because *Tbr2* is expressed in all IPs, our approach using *Tbr2*^{CreER} for lineage tracing could not distinguish among IP subtypes, and further studies will be necessary to test whether different groups of IPs (e.g. Pax6^{+} and Pax6^{-}) produce distinct clonal profiles. Other possibilities to explain variations in clone size are that IPs re-enter the cell cycle stochastically, or under the influence of other intrinsic or extrinsic factors.

The extensive apoptosis of early IP primary daughter cells, observed in ∼2/3 of clones overall, raises the possibility that many IPs, especially those destined for further proliferation, undergo binary cell death decisions linked to asymmetric cell division. Binary cell death mechanisms have been described in many systems, such as *Drosophila* sensory organ lineages (Orgogozo et al., 2002). Binary cell death decisions can be regulated by the unequal segregation of Numb or other molecules related to Notch signaling at mitosis (Arya and White, 2015; Yamaguchi and Miura, 2015). However, it is presently unclear why proliferation or differentiation of one IP daughter cell should be linked to death of the other daughter cell. Observations of microglia in the VZ/SVZ of embryonic neocortex, including microglia that have ingested Tbr2^{+} nuclei, denote the likely involvement of microglia in this process (Cunningham et al., 2013; Tronnes et al., 2016).

MATERIALS AND METHODS

Animals and tissue collection

C57BL/6 and CD1 mice used in this study were kept in a 12 h light/dark cycle, with food and water *ad libitum*, in the Seattle Children's Research Institute (SCRI) vivarium. All animal experimental procedures were performed with approval of the SCRI Institutional Animal Care and Use Committee. All procedures followed guidelines outlined in the National Research Council Guide for the Care and Use of Laboratory Animals. The following previously described mouse transgenic alleles were used: *Eomes*^{CreERT2} (Pimeisl et al., 2013), MADM-11GT and MADM-11TG (Hippenmeyer et al., 2010). MADM-11GT (C56BL/6) and MADM-11TG (CD1) mice are available at The Jackson Laboratory Repository (http://jaxmice.jax.org/query) under JAX Stock No. 013749 (MADM-11-GT) and JAX Stock No. 013751 (MADM-11-TG). For clonal analysis, male mice with *Eomes*$^{CreERT2/+}$; *Madm11*$^{GT/GT}$ were bred with female *Madm11*$^{TG/TG}$ mice. The day of the vaginal plug was considered as E0.5. Pregnant dams were anesthetized with isoflurane (Patterson Vet) and killed by cervical dislocation, after which embryos were harvested. Embryos (male and female) were decapitated, and brains were fixed in 4% (wt/vol) paraformaldehyde (PFA) in 0.1 M sodium phosphate (pH 7.4) at 4°C for 4 h. Fixed brains were cryoprotected in 30% (wt/vol) sucrose in PBS, frozen in optimum cutting temperature compound (OCT; Sakura Finetek), cryosectioned at 30 µm and mounted on Superfrost Plus slides (12-550-15, Thermo Fisher Scientific). Slide-mounted sections were stored at −80°C until needed.

Tamoxifen administration

Pregnant dams were administered tamoxifen (T5648, Sigma-Aldrich; 30-75 mg/kg) and progesterone (P3972, Sigma-Aldrich; 15-38 mg/kg) by intraperitoneal injection, at the indicated embryonic ages.

Image acquisition and clone reconstruction

Confocal *Z* stacks were acquired with a Zeiss LSM-710 confocal microscope with Zen acquisition software. 3D reconstructions of *Z* stacks were concatenated for clones spanning several 30 µm adjacent sections using NIH ImageJ software (https://imagej.nih.gov/ij/). Images were adjusted for contrast and brightness in Adobe Photoshop. All sections containing cortex within a brain were screened for labeled cells to ensure that all cells within a single clone spanning several sections were taken into account. Data were reported as mean±s.e.m. from at least 3 brains per data point.

NND analysis

NNDs were analyzed as previously described (Brown et al., 2011; Gao et al., 2014), using Python. NND distribution reflects the spatial cell pattern within a given data set. For a given data set, the distance of each cell i to its closest neighbor (NND) was measured and denoted as d_i. The indicator function $f(y, d)$ was calculated as:

$$f(y,\ d) = f(x) = \begin{cases} 1, & \text{if } d \le y, \\ 0, & \text{otherwise}. \end{cases}$$

The cumulative distribution function of NND is:

$$G(y) = \sum_{i=1}^{N} f(y,\ \mathrm{di}).$$

Shorter NNDs reflect clustering, whereas the longer NNDs reflect dispersion of cells. Simulated random data sets contained the same number of data points within the same volume as the experimental data sets and were repeated 100 times. Statistical analysis used 2-sample Kolmogorov–Smirnov test between cumulative percentage distribution of each clone and the mean for its corresponding simulated random data sets.

Acknowledgements

We thank Dr Simon Hippenmeyer for helpful discussions, and Dr Stefan Mihalas for help with NND analysis.

Competing interests

The authors declare no competing or financial interests.

Author contributions

Conceptualization: A.M., R.F.H.; Methodology: A.M., R.F.H.; Formal analysis: A.M., R.F.H.; Investigation: A.M.; Data curation: A.M.; Writing - original draft: A.M.; Writing - review & editing: A.M., R.F.H.; Visualization: A.M., R.F.H.; Supervision: R.F.H.; Funding acquisition: R.F.H.

Funding

This work was supported by the National Institutes of Health [NS092339 and NS085081 to R.F.H.]. Deposited in PMC for release after 12 months.

Supplementary information

Supplementary information available online at
http://dev.biologists.org/lookup/doi/10.1242/dev.164335.supplemental

References

Arya, R. and White, K. (2015). Cell death in development: signaling pathways and core mechanisms. *Semin. Cell Dev. Biol.* **39**, 12-19.

Blaschke, A. J., Staley, K. and Chun, J. (1996). Widespread programmed cell death in proliferative and postmitotic regions of the fetal cerebral cortex. *Development* **122**, 1165-1174.

Brown, K. N., Chen, S., Han, Z., Lu, C.-H., Tan, X., Zhang, X.-J., Ding, L., Lopez-Cruz, A., Saur, D., Anderson, S. A. et al. (2011). Clonal production and organization of inhibitory interneurons in the neocortex. *Science* **334**, 480-486.

Caviness, V. S., Jr, Goto, T., Tarui, T., Takahashi, T., Bhide, P. G. and Nowakowski, R. S. (2003). Cell output, cell cycle duration and neuronal specification: a model of integrated mechanisms of the neocortical proliferative process. *Cereb. Cortex* **13**, 592-598.

Cunningham, C. L., Martinez-Cerdeno, V. and Noctor, S. C. (2013). Microglia regulate the number of neural precursor cells in the developing cerebral cortex. *J. Neurosci.* **33**, 4216-4233.

Desai, A. R. and McConnell, S. K. (2000). Progressive restriction in fate potential by neural progenitors during cerebral cortical development. *Development* **127**, 2863-2872.

Eckler, M. J., Nguyen, T. D., McKenna, W. L., Fastow, B. L., Guo, C., Rubenstein, J. L. R. and Chen, B. (2015). Cux2-positive radial glial cells generate diverse subtypes of neocortical projection neurons and macroglia. *Neuron* **86**, 1100-1108.

Englund, C., Fink, A., Lau, C., Pham, D., Daza, R. A., Bulfone, A., Kowalczyk, T. and Hevner, R. F. (2005). Pax6, Tbr2, and Tbr1 are expressed sequentially by radial glia, intermediate progenitor cells, and postmitotic neurons in developing neocortex. *J. Neurosci.* **25**, 247-251.

Florio, M. and Huttner, W. B. (2014). Neural progenitors, neurogenesis and the evolution of the neocortex. *Development* **141**, 2182-2194.

Franco, S. J., Gil-Sanz, C., Martinez-Garay, I., Espinosa, A., Harkins-Perry, S. R., Ramos, C. and Muller, U. (2012). Fate-restricted neural progenitors in the mammalian cerebral cortex. *Science* **337**, 746-749.

Gao, P., Postiglione, M. P., Krieger, T. G., Hernandez, L., Wang, C., Han, Z., Streicher, C., Papusheva, E., Insolera, R., Chugh, K. et al. (2014). Deterministic progenitor behavior and unitary production of neurons in the neocortex. *Cell* **159**, 775-788.

Gil-Sanz, C., Espinosa, A., Fregoso, S. P., Bluske, K. K., Cunningham, C. L., Martinez-Garay, I., Zeng, H., Franco, S. J. and Müller, U. (2015). Lineage tracing using Cux2-Cre and Cux2-CreERT2 mice. *Neuron* **86**, 1091-1099.

Guo, C., Eckler, M. J., McKenna, W. L., McKinsey, G. L., Rubenstein, J. L. R. and Chen, B. (2013). Fezf2 expression identifies a multipotent progenitor for neocortical projection neurons, astrocytes, and oligodendrocytes. *Neuron* **80**, 1167-1174.

Hevner, R. F., Daza, R. A., Rubenstein, J. L. R., Stunnenberg, H., Olavarria, J. F. and Englund, C. (2003). Beyond laminar fate: toward a molecular classification of cortical projection/pyramidal neurons. *Dev. Neurosci.* **25**, 139-151.

Hevner, R. F., Daza, R. A. M., Englund, C., Kohtz, J. and Fink, A. (2004). Postnatal shifts of interneuron position in the neocortex of normal and *reeler* mice: evidence for inward radial migration. *Neuroscience* **124**, 605-618.

Hevner, R. F., Hodge, R. D., Daza, R. A. M. and Englund, C. (2006). Transcription factors in glutamatergic neurogenesis: conserved programs in neocortex, cerebellum, and adult hippocampus. *Neurosci. Res.* **55**, 223-233.

Hippenmeyer, S., Youn, Y. H., Moon, H. M., Miyamichi, K., Zong, H., Wynshaw-Boris, A. and Luo, L. (2010). Genetic mosaic dissection of Lis1 and Ndel1 in neuronal migration. *Neuron* **68**, 695-709.

Hoerder-Suabedissen, A. and Molnár, Z. (2013). Molecular diversity of early-born subplate neurons. *Cereb. Cortex* **23**, 1473-1483.

Kaplan, E. S., Ramos-Laguna, K. A., Mihalas, A. B., Daza, R. A. M. and Hevner, R. F. (2017). Neocortical Sox9+ radial glia generate glutamatergic neurons for all layers, but lack discernible evidence of early laminar fate restriction. *Neural Dev.* **12**, 14.

Kawaguchi, A., Ikawa, T., Kasukawa, T., Ueda, H. R., Kurimoto, K., Saitou, M. and Matsuzaki, F. (2008). Single-cell gene profiling defines differential progenitor subclasses in mammalian neurogenesis. *Development* **135**, 3113-3124.

Kowalczyk, T., Pontious, A., Englund, C., Daza, R. A., Bedogni, F., Hodge, R., Attardo, A., Bell, C., Huttner, W. B. and Hevner, R. F. (2009). Intermediate neuronal progenitors (basal progenitors) produce pyramidal-projection neurons for all layers of cerebral cortex. *Cereb. Cortex* **19**, 2439-2450.

Leone, D. P., Srinivasan, K., Chen, B., Alcamo, E. and McConnell, S. K. (2008). The determination of projection neuron identity in the developing cerebral cortex. *Curr. Opin. Neurobiol.* **18**, 28-35.

Luskin, M. B., Pearlman, A. L. and Sanes, J. R. (1988). Cell lineage in the cerebral cortex of the mouse studied in vivo and in vitro with a recombinant retrovirus. *Neuron* **1**, 635-647.

McConnell, S. K. (1985). Migration and differentiation of cerebral cortical neurons after transplantation into the brains of ferrets. *Science* **229**, 1268-1271.

McConnell, S. K. and Kaznowski, C. E. (1991). Cell cycle dependence of laminar determination in developing neocortex. *Science* **254**, 282-285.

Mihalas, A. B., Elsen, G. E., Bedogni, F., Daza, R. A. M., Ramos-Laguna, K. A., Arnold, S. J. and Hevner, R. F. (2016). Intermediate progenitor cohorts differentially generate cortical layers and require Tbr2 for timely acquisition of neuronal subtype identity. *Cell Rep.* **16**, 92-105.

Noctor, S. C., Martínez-Cerdeño, V., Ivic, L. and Kriegstein, A. R. (2004). Cortical neurons arise in symmetric and asymmetric division zones and migrate through specific phases. *Nat. Neurosci.* **7**, 136-144.

Orgogozo, V., Schweisguth, F. and Bellaiche, Y. (2002). Binary cell death decision regulated by unequal partitioning of Numb at mitosis. *Development* **129**, 4677-4684.

Pimeisl, I. M., Tanriver, Y., Daza, R. A., Vauti, F., Hevner, R. F., Arnold, H. H. and Arnold, S. J. (2013). Generation and characterization of a tamoxifen-inducible Eomes(CreER) mouse line. *Genesis* **51**, 725-733.

Shen, Q., Wang, Y., Dimos, J. T., Fasano, C. A., Phoenix, T. N., Lemischka, I. R., Ivanova, N. B., Stifani, S., Morrisey, E. E. and Temple, S. (2006). The timing of cortical neurogenesis is encoded within lineages of individual progenitor cells. *Nat. Neurosci.* **9**, 743-751.

Thomaidou, D., Mione, M. C., Cavanagh, J. F. R. and Parnavelas, J. G. (1997). Apoptosis and its relation to the cell cycle in the developing cerebral cortex. *J. Neurosci.* **17**, 1075-1085.

Tronnes, A. A., Koschnitzky, J., Daza, R., Hitti, J., Ramirez, J. M. and Hevner, R. (2016). Effects of lipopolysaccharide and progesterone exposures on embryonic cerebral cortex development in mice. *Reprod. Sci.* **23**, 771-778.

Vasistha, N. A., García-Moreno, F., Arora, S., Cheung, A. F. P., Arnold, S. J., Robertson, E. J. and Molnár, Z. (2015). Cortical and clonal contribution of Tbr2 expressing progenitors in the developing mouse brain. *Cereb. Cortex* **25**, 3290-3302.

Walsh, C. and Cepko, C. L. (1988). Clonally related cortical cells show several migration patterns. *Science* **241**, 1342-1345.

Wu, S.-X., Goebbels, S., Nakamura, K., Nakamura, K., Kometani, K., Minato, N., Kaneko, T., Nave, K. A. and Tamamaki, N. (2005). Pyramidal neurons of upper cortical layers generated by NEX-positive progenitor cells in the subventricular zone. *Proc. Natl. Acad. Sci. USA* **102**, 17172-17177.

Yamaguchi, Y. and Miura, M. (2015). Programmed cell death in neurodevelopment. *Dev. Cell* **32**, 478-490.

Figure S1

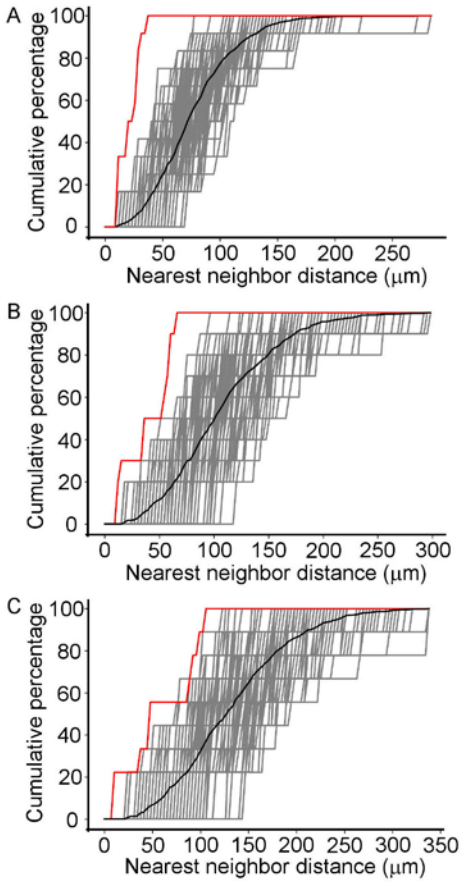

Figure S1. Nearest neighbor distance (NND) analysis of multilayer clones. (A-C) Plots represent the cumulative percentage distribution of NNDs of three individual multilayer clones (red) and corresponding random simulated data sets (gray for each set, black for the mean of all sets). The data indicate that labeled neurons were not randomly distributed, but formed clusters consistent with clonal origins. (A) An E11.5 IP clone; $p = 2.4\text{x}10^{-9}$. (B) An E11.5 IP clone (shown in Fig. 1C-C"); $p = 2.1\text{x}10^{-6}$. (C) An E13.5 IP clone; $p = 4.6\text{x}10^{-04}$.